Helical Stability of *de Novo* Designed α-Aminoisobutyric Acid-Rich Peptides at High Temperatures†

J. D. Augspurger, V. A. Bindra, H. A. Scheraga, and A. Kuki*

Baker Laboratory of Chemistry, Cornell University, Ithaca, New York 14853-1301

Received May 19, 1994; Revised Manuscript Received September 20, 1994®

ABSTRACT: 1D and 2D NMR spectroscopy is used to determine the helical stability of two Aib-rich peptides, ^{t}Boc-(Aib)$_3$-DkNap-Leu-Aib-Ala-(Aib)$_2$-NH(CH$_2$)$_2$OCH$_3$ (Dk^4[7/9]) and Ac-(Aib)$_2$-β-(1′-naphthyl)Ala-(Aib)$_2$-Phe-(Aib)$_2$-NHMe (Nap^{3}Phe^6[6/8]), where the bracket notation indicates the number of Aib-class residues/total number of residues. 2D ROESY experiments, carried out previously on Nap^{3}Phe^6[6/8] in DMSO (Basu & Kuki, 1993), showed that this compound adopts the 3_{10}-helical conformation at 20 °C. The first step in the present work is to apply this technique to the peptide Dk^4[7/9], demonstrating that it likewise adopts the 3_{10}-helical conformation in chloroform at 20 °C. The amide proton shifts of Nap^3-Phe^6[6/8] in DMSO and Dk^4[7/9] in $C_2D_2Cl_4$ were then monitored by means of 1D NMR over a large temperature range, up to 150 and 120 °C, respectively. The nonamer Dk^4[7/9] exhibits no evidence of any conformational or unfolding transition as the temperature is raised. The nearly temperature independent amide proton chemical shifts of this nonamer are an indication of retention of the intrahelical hydrogen bonding, which was then verified directly by solvent perturbation with DMSO at 120 °C. The resulting hydrogen-bonding pattern confirms that Dk^4[7/9] retains its 3_{10}-helical conformation in $C_2D_2Cl_4$ over the entire temperature range. This conformational quietness is exploited to examine the intrinsic temperature dependence of free versus intrahelically hydrogen bonded amide proton shifts within the same peptide structure. It is also shown that Nap^{3}Phe^6[6/8] retains its 3_{10}-helical conformation over the entire temperature range in the stronger hydrogen-bonding solvent DMSO. The extreme thermal stability of these octameric and nonameric Aib-rich peptides in both solvents is contrasted with that of much longer alanine-rich peptides in water.

The relative helix-forming propensity of amino acids has long been a subject of considerable interest (Altmann et al., 1990; Wójcik et al., 1990; and references therein) and has also been the focus of a number of recent studies (O'Neil & DeGrado, 1990; Hermans et al., 1992). While the stability of helical backbone structures in folded proteins involves large favorable contributions from the packing and hydrophobic core constraints of the full three-dimensional structure, it is in the quantitative investigation of single helical peptides that the conformational determinants of regular backbone structure formation and stability may be isolated. Since the demonstration of significant α-helix content of a predominantly alanine-containing oligopeptide of 16 residues at low temperatures by Marqusee and Baldwin (1987) and Marqusee et al. (1989), the helix content of many *de novo* designed oligopeptides has been studied (Bradley et al., 1990; Merutka & Stellwagon, 1989, 1990; Merutka et al., 1993; Liff et al., 1991; Scholtz et al., 1991a,b, 1993; Rohl et al., 1992; Vila et al., 1992; Chakrabartty et al., 1994).

α-Aminoisobutyric acid (Aib, or α-methylalanine) has been reported to possess a slightly greater intrinsic helix-forming capacity than alanine (O'Neil & DeGrado, 1990; Hermans et al., 1992), when added as an isolated residue in systematic studies of guest amino acids incorporated into oligopeptide sequences at room temperature. Of the different guests reported in these series, Aib is indeed found to be the amino acid with the maximum stabilization of the helix/coil equilibrium constant. While Aib is a nonprotein amino acid, it is the protypical α,α-dialkylated amino acid which has been found in a diversity of natural peptides, particularly of microbial origin (Prasad & Balaram, 1984). Interest in the steric hindrance arising from the *gem*-dimethyl group has led to extensive prior studies at the other end of the composition spectrum, i.e., 100% Aib. Pure Aib homo-oligomers, scrutinized by theoretical (Paterson et al., 1981), solution phase (Toniolo et al., 1985), and crystallographic (Toniolo et al., 1991) methods, have been extensively documented as forming exclusively helical backbone structures and in particular 3_{10}-helices. Theoretical modeling of the relative free energies of the 3_{10}- vs α-helical regular backbone structures has also been pursued in extensive simulations (Huston & Marshall, 1994) and with inclusion of solvent (Smythe et al., 1993).

It is, however, in the intermediary composition range, in natural and synthetic peptides, where the most revealing tests have been developed. These studies have demonstrated the ability of Aib to stabilize helices of diverse sequences. As documented in the review by Karle and Balaram (1990), predictable 3_{10}-helicity results when the Aib composition exceeds 50%, with sole deviations due to contiguous pairs or triplets of non-Aib residues, as demonstrated in sequences studied elsewhere (Balaram et al., 1986; Basu et al., 1991). When the Aib content is lowered by dilution with common L-amino acids (mono-α-alkylated amino acids) to 50% composition or below, a complex and subtle behavior arises (Karle & Balaram, 1990; DiBlasio et al., 1993). We have

† This work was supported by research grants from the National Institute of General Medical Sciences [GM-24893 (H.A.S.) and GM-39576 (A.K.)] of the National Institutes of Health.

® Abstract published in *Advance ACS Abstracts,* February 1, 1995.

0006-2960/95/0434-2566$09.00/0

termed this behavior pattern "ambihelicity" (Basu et al., 1991), in which the α-helical and 3_{10}-helical forms are nearly of equivalent energy, mixed $3_{10}/\alpha$-helical structures can occur, and prediction is subtle (Marshall et al., 1990; Basu & Kuki, 1992). Nevertheless, such Aib-containing sequences are invariably helical.

In our research program, we have chosen to map the sequence terrain of >50% Aib-rich sequences (Basu et al., 1991, 1993) containing only isolated noncontiguous L-amino acids, with the aim to prepare a single helical form reliably [3_{10}; see Figure 1 of Karle and Balaram (1990)]. When incorporating aromatic guest residues of synthetic origin, we have focused on a new type known as ≥70% Aib-class sequences, where "Aib class" includes not only Aib but certain other α,α-dialkylated amino acids designed to share the Aib helical propensity (Bindra & Kuki, 1994).[1] In this report we will examine the 3_{10}-helicity over a range of temperatures, in order to explore the thermodynamic characterization and high-temperature stability of the helical structure in two such Aib-rich peptide sequences. The octamer Ac-$(Aib)_2$-β-(1′-naphthyl)Ala-$(Aib)_2$-Phe-$(Aib)_2$-NHMe, Nap^{3}Phe^6[6/8] [previously referred to as 3,6-NF by Basu et al. (1991)], where the [6/8] notation indicates that six of the eight residues are Aib class, has been shown to form 3_{10}-helices at room temperature (Basu & Kuki, 1993). The Aib-rich nonamer ^{t}Boc-$(Aib)_3$-DkNap-Leu-Aib-Ala-$(Aib)_2$-$NHCH_2CH_2OCH_3$, denoted as Dk^4[7/9], possesses seven Aib-class amino acids—six Aib residues and a diketonaphthylamino acid, DkNap (Kotha et al., 1992)—out of a total of nine amino acids. A schematic representation of the three-dimensional structure of Dk^4[7/9], including the DkNap side chain, is given in Figure 1. Preliminary results indicate that this Aib-rich nonamer likewise forms 3_{10}-helices at room temperature (Bindra & Kuki, 1994). In a behavior pattern typical of a 3_{10}-helix, two, and only two, amide protons were found to be free (not intrahelically hydrogen bonded). The terminal blocking groups were chosen to provide the hydrogen-bonding CO group (Ac and ^{t}Boc) and NH group (methylamine and 2-methoxyethylamine), with enhanced solubility provided by the larger flexible blocking groups.

The 3_{10}-helical conformation of Dk^4[7/9] is first confirmed by means of 2D NMR spectroscopy. In general, 2D NMR methods have not been used for Aib peptides because their amide protons cannot participate in scalar coupling due to the absence of α-hydrogens. However, the peptides here are designed to carry an NMR handle consisting of a few selected L-residues positioned to yield maximum structural information. Such methods for applying 2D NMR ROESY to peptides rich in Aib amino acids have been developed (Slomczynska et al., 1992; Basu & Kuki, 1993) and applied to Nap^{3}Phe^6[6/8]. A complete set of helical NN and αN correlations was observed (Basu & Kuki, 1993). In combination with the assignment of hydrogen-bonded and free backbone amides, that NMR study proved that Nap^{3}Phe^6-[6/8] was 3_{10}-helical and not α-helical.

We next increase the temperature in an attempt to locate a melting transition and thereby to develop a measure of the helical stability in these Aib-rich designs. Both the octamer Nap^{3}Phe^6[6/8] and the nonamer Dk^4[7/9] were studied at elevated temperatures, up to 150 °C in DMSO and 120 °C in $C_2D_2Cl_4$, respectively. The results on the thermal stability of the folded helices and the interpretation of their temperature-dependent NMR form the central findings of this work.

The temperature coefficient method—monitoring the slopes of the chemical shift vs temperature in a strong hydrogen-bonding solvent such as DMSO-d_6 (Pitner & Urry, 1972)—is a well-established method for determining hydrogen bonding. What has been less clear is the interpretation and significance of a temperature dependence study in a weakly polar solvent such as $CDCl_3$ or $C_2D_2Cl_4$. Temperature-dependent NMR spectra were recorded over a wide temperature range in both types of solvent, and comparison is made between the temperature dependence of intrahelically hydrogen-bonded and free amide protons in the weakly polar solvent. The intrinsic temperature dependence of these two types of amide proton chemical shifts within a single regular backbone structure is examined. These observations would not have been possible in a more typical and dynamically active multiple-conformation peptide system but are possible in the remarkably conformationally "quiet" Aib-rich peptide systems, as detailed below.

EXPERIMENTAL PROCEDURES

The syntheses of Nap^{3}Phe^6[6/8] and Dk^4[7/9] have been described previously (Basu et al., 1991; Bindra & Kuki, 1994). The peptides were purified by reverse-phase HPLC (Waters prep-Nova-Pak C_{18} column) with 5−10% H_2O in MeOH as eluent. The deuterated solvents were used as received. Deuterated chloroform (99.8%) was obtained from Aldrich Laboratories. Deuterated DMSO and 1,1,2,2-tetrachloroethane (99.9% D and 99.6% D), respectively, were obtained from Cambridge Isotope Laboratories.

The molecular weight of Dk^4[7/9] falls in the range (around 1000) where the nuclear Overhauser effects (NOEs) are very weak at the general magnetic field strength usually employed. This is due to the size of the molecule, which has a molecular tumbling time, τ_c, close to $1/\omega_L$, where ω_L is the angular proton Larmor frequency. Because of the dependence of spin relaxation kinetics on τ_c the 2D NOESY experiment, which normally provides valuable "through-space connectivity", often gives poor results for molecules with molecular weights around 1000. Here, the spin-locked NOE experiment (Bothner-By et al., 1984) is a far more effective method for obtaining NOE information. Intensities of NOE peaks in a ROESY experiment are known to be less sensitive to the value of the correlation time (Bothner-By et al., 1984). Artifacts induced by the homonuclear Hartmann−Hahn effect are minimized by using a relatively weak rf field and positioning the carrier frequency in the downfield region of the spectrum.

DQF-COSY (Piantini et al., 1982) and ROESY (Bothner-By et al., 1984; Bax & Davis, 1985) spectra of Dk^4[7/9] were obtained in $CDCl_3$ at 20 °C. The ROESY spectrum in $CDCl_3$ was obtained at mixing times of 60, 130, 250, 370, and 500 ms. ROESY was carried out on a Varian Unity 500 spectrometer in $CDCl_3$ at 20 °C with a peptide concentration of 4 mg/mL. The ROESY spectrum was recorded with 256 t_1 experiments of eight scans with a 2-s relaxation delay and 0.146-s acquisition time. A homospoil−90−homospoil sequence preceded the delay. The strong cross-peaks shown and analyzed were obtained with a mixing time (τ_m) of 370 ms, during which the effective field strength

[1] This paper contains the definition of "Aib class" and of the [7/9] nomenclature system for Aib-class peptides.

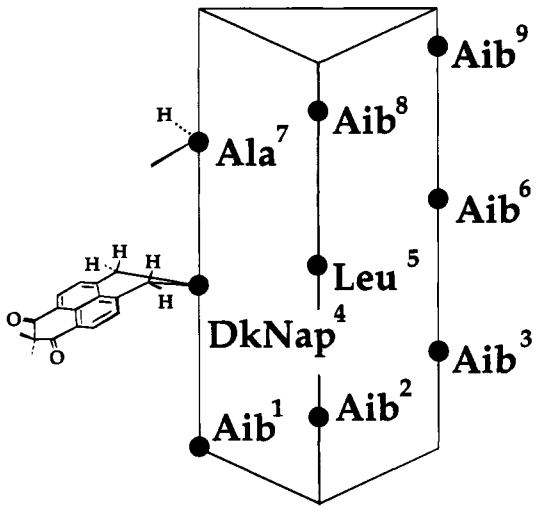

FIGURE 1: Schematic 3_{10}-prism representation of the three-dimensional structure of the right-handed 3_{10}-helix of the nonamer Dk⁴[7/9], with the orientation of the DkNap side chain indicated.

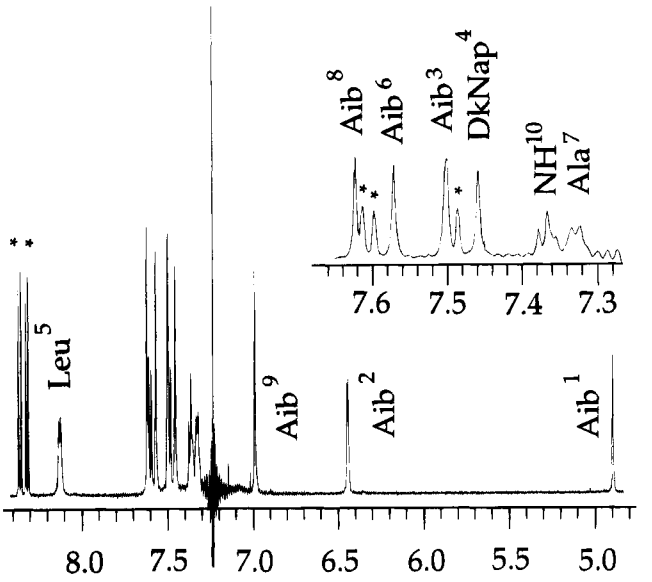

FIGURE 2: 1D NMR spectrum at 500 MHz in $CDCl_3$ at 20 °C of the amide and aromatic proton region of Dk⁴[7/9]. The asterisks indicate resonances arising from the aromatic protons of the DkNap residue.

was 4.0 kHz. The spin locking was achieved by a series of hard pulses of 30° flip angles with resonance offset compensation achieved by two flanking 90° hard pulses about the spin lock. The transmitter offset was placed at 5.2 ppm during the experiment, and a spectral width of 7000.4 Hz was used in both dimensions. The 2048 × 256 data matrix was zero filled at 4K × 4K before any further processing.

1D NMR spectra of Nap³Phe⁶[6/8] and Dk⁴[7/9] were also taken over a large temperature range on a Varian 400-MHz spectrometer. The solvent for Nap³Phe⁶[6/8] was DMSO-d_6, as in previous work (Basu et al., 1991), and proton chemical shifts were referenced to the uncorrected residual solvent peak (2.49 ppm). While the previous work on Dk⁴-[7/9] was carried out in $CDCl_3$, its low boiling point makes it unsuitable for the temperature range that we desired to explore. Hence, deuterated 1,1,2,2-tetrachloroethane was utilized as the solvent for Dk⁴[7/9], and again the uncorrected residual solvent peak was used as the reference (5.98 ppm). Samples were prepared at 1 mg/mL concentration to ensure that any aggregation effects on the chemical shifts would be negligible. As previously reported (Bindra & Kuki, 1994), both concentration-dependent and DMSO-dependent studies were carried out at room temperature, which verified that the observed hydrogen-bonding pattern arises from monomeric helices.

In addition, a solvent perturbation study was carried out by means of 1D NMR at 500 MHz on Dk⁴[7/9] in the $C_2D_2Cl_4$ system directly at the high-temperature end of the $C_2D_2Cl_4$ range, 120 °C. A 600-μL NMR sample was prepared in $C_2D_2Cl_4$, and measured amounts of DMSO-d_6 were added, up to a final solution of nearly 20% DMSO (by volume).

RESULTS

Sequential Correlations and Helicity. The peptide Dk⁴-[7/9] has ten amide protons: six singlets from Aib residues, one singlet from the DkNap residue (see side chain diagramed in Figure 1), two doublets from the Leu and the Ala residues, and one triplet from the NH of the C-terminal blocking group $NHCH_2CH_2OCH_3$. The assignments in $CDCl_3$ have been described in a previous report (Bindra & Kuki, 1994) and are given along with the aromatic resonances from DkNap in Figure 2 and Table 1. Figure 3 is a schematic representation of the peptide showing the sequence and its numbering. The Leu⁵ (8.119 ppm) and the Ala⁷ (7.335 ppm) amide resonances and the amide triplet (7.376 ppm) of the NH of the $NHCH_2CH_2OCH_3$ protecting group are the only peaks assignable by normal scalar coupling methods.

Table 1: Amide Proton Shifts (ppm) of Dk⁴[7/9] at 20 °C

		$C_2D_2Cl_4$	
resonance	$CDCl_3$[a] δ (ppm)	δ (ppm)	$\Delta\delta/\Delta T$[b]
NH^{10}	7.376	7.261	−0.9
Aib^9	7.003	6.993	−1.0
Aib^8	7.623	7.631[c]	−1.6[c]
Ala^7	7.335	7.267	−0.9
Aib^6	7.578	7.530[c]	−0.6[c]
Leu^5	8.119	8.123	−1.2
$DkNap^4$	7.452	7.473, 7.473[d]	−1.8, −1.6[d]
Aib^3	7.495		
Aib^2	6.427	6.346	−0.3
Aib^1	4.882	4.772	−0.5

[a] Bindra and Kuki (1994). The behavior pattern indicative of a 3_{10}-helix was observed at 20 °C: two, and only two, amide protons are free (not intrahelically hydrogen bonded), and upon assignment these NH resonances were determined to be those of Aib^1 and Aib^2, as required for the 3_{10}-helix. [b] The temperature coefficient, normally defined as $d\delta/dT$, is given here by the finite difference, $\Delta\delta/\Delta T = [\delta(120\ °C) - \delta(20\ °C)]/100\ °C$ (in ppb/°C). [c] These two chemical shifts were too close to assign definitively by comparison to the $CDCl_3$ spectrum. However, the reverse assignment of that shown would require a crossover and a larger change in the chemical shift between the two solvents than that shown; hence, the assignment was made on this basis. The assignment of these two shifts is not crucial to the analysis. [d] These two resonances were unresolvable at 400 MHz in $C_2D_2Cl_4$ at 20 °C and thus are not separately assignable. Again, assignment of these two shifts is not crucial to the analysis of chemical shift behavior.

Figure 4 shows the correlation of aromatic and amide resonances with $C^{\alpha}H$ and $C^{\beta}H$ resonances. The $d_{\alpha N}(i,i+1)$ are sufficiently short to produce a cross-peak for the entire range of backbone dihedral angles ψ_i (Wüthrich, 1986) and hence enabled the assignment of the Aib amides immediately following the two L-amino acids Leu^5 (Aib^6) and Ala^7 (Aib^8). The $d_{NN}(i,i+1)$, on the other hand, is a function of the intervening dihedral angles ϕ_i and ψ_i and varies between the

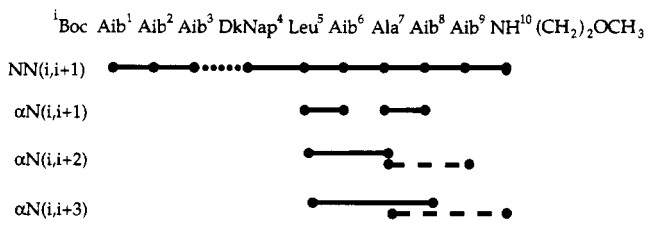

FIGURE 3: A summary of the observed NOE correlations of the backbone protons of Dk[4][7/9]. Solid lines indicate NOEs which were clearly evident. It should be noted that the strong NN(i,i+1) correlations extend from the N-terminus to the C-terminus of the peptide, with the exception of NN(3,4), which is obscured by its extreme closeness to the diagonal. Broken lines indicate NOEs which are suggested by the data but are weak. NN(i,i+2) correlations are not observed. The observation of αN(i,i+2) and αN(i,i+3), but not αN(i,i+4), correlations is characteristic of a 3_{10}-helix.

van der Waals limit of 2.0 Å and approximately 4.7 Å. For a helical backbone, whether 3_{10}- or α-helical, a characteristic sequence of connected NN(i,i+1) NOE signals arises with sequential $d_{NN}(i,i+1)$ distances between 2.6 and 2.8 Å (Wüthrich, 1986); thus, we examined the ROESY spectrum of Dk[4][7/9] for such a complete sequence. The corresponding region of the spectrum containing correlations among the amide and the aromatic DkNap resonances is shown in Figure 5. All amide resonances except one (because of the extreme closeness to the diagonal, DkNap[4]NH at 7.452 ppm and Aib[3] at 7.495 ppm) are indeed observed to be correlated in a complete sequence. This, in combination with the hydrogen-bonding data (Bindra & Kuki, 1994), is strong evidence of a helical conformation along the entire length (Figure 5).

3_{10}-Helix vs α-Helix. The relatively large NN(i,i+1) cross-peak intensities for amides four through ten are indicative of a stable helical structure, rather than any more conformationally mobile form (see Table 2). The relative magnitudes of the cross-peak intensities for amides one through three, namely, for Aib[1]NH−Aib[2]NH and Aib[2]NH−Aib[3]NH, are weaker than the remaining amide cross-peaks. This may be significant, since an α-helix, or a conformational distribution including both 3_{10}-helical and α-helical minima, would require a completely free or weakened Aib[3]NH, respectively. However, in the previous solvent perturbation study of the amides in Dk[4][7/9] (Bindra & Kuki, 1994), Aib[1]NH and Aib[2]-NH were found to be the solvent-exposed NH protons, while Aib[3]NH showed the fully characteristic solvent perturbation insensitivity of an intramolecularly hydrogen-bonded amide. This is reconfirmed below for Dk[4][7/9] at a much higher temperature. Hence, the weaker NN(i,i+1) cross-peaks do not arise from weakened hydrogen bonding of Aib[3]NH but rather could simply reflect the greater fluctuations in $d_{NN}(i,i+1)$ due to motion of the non-hydrogen-bonded Aib[1]NH and Aib[2]NH within the 3_{10}-helical hydrogen-bonded structure. In addition, medium-range NOE correlations are also observed which provide independent evidence pertinent to the establishment of 3_{10}- vs α-helicity.

The medium-range distances expected in helical peptides—$d_{\alpha N}(i,i+2)$, $d_{NN}(i,i+2)$, $d_{\alpha N}(i,i+3)$, and $d_{\alpha N}(i,i+4)$—give rise to weaker but observable NOEs and have been observed in other Aib-rich peptides (Slomczynska et al., 1992; Basu & Kuki, 1993). Those which were observed for Dk[4][7/9] due to correlations with the α-proteins of Leu[5] and Ala[7] are shown in Figure 4.

Among these distances, short $d_{\alpha N}(i,i+3)$ is uniquely characteristic of helical conformations (both the 3_{10}- and α-helix) and does not occur in other regular backbone structures. The nonsequential (i,i+3) cross-peak between

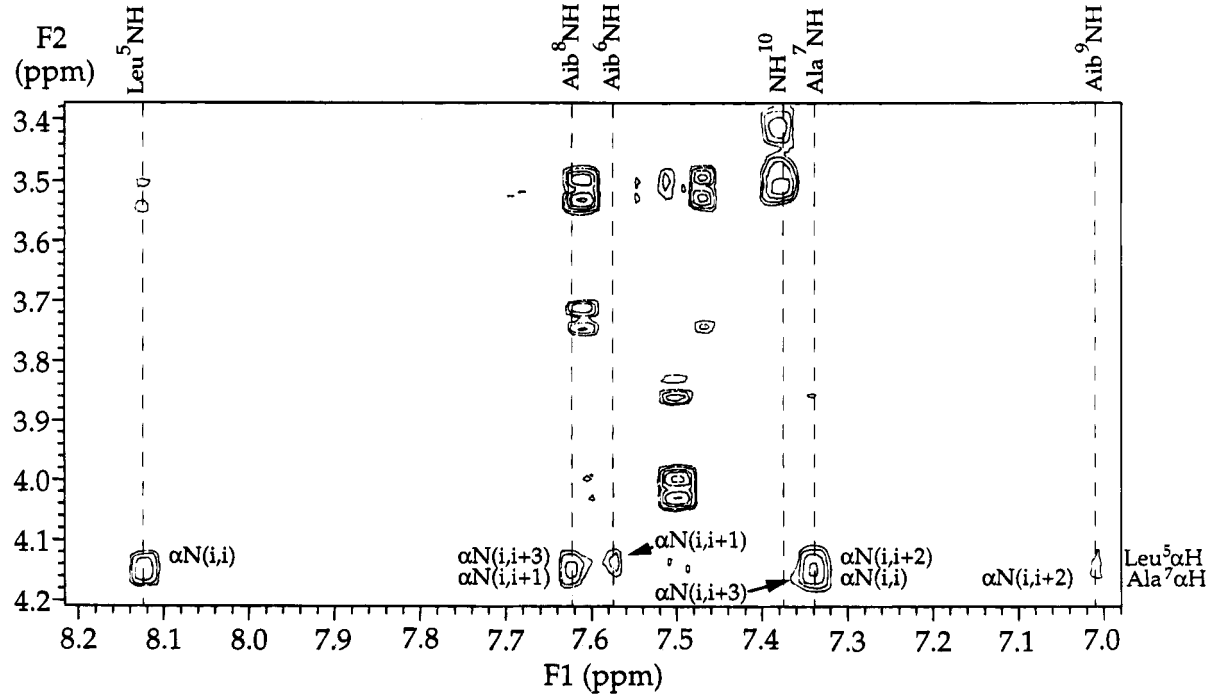

FIGURE 4: Selected section of the 500-MHz 2D ROESY spectrum of Dk[4][7/9] in $CDCl_3$ at 20 °C showing correlations of amide and aromatic protons with the $C^{\alpha}H$ and $C^{\beta}H$ resonances. All of these cross-peaks are negative with respect to the diagonal. The locations of the amide proton resonances are indicated along the F_1 axis and those of the $C^{\alpha}H$ along the F_2 axis. The correlations with aliphatic methylenes, resonances between 3.4 and 4.1 ppm, are intraresidue correlations in DkNap and the C-terminal blocking group. In the 4.1−4.2 ppm region, the small separation between the Leu[5]$C^{\alpha}H$ and Ala[7]$C^{\alpha}H$ resonances leads to overlap between cross-peaks. However, the non-nearest-neighbor αN(i,i+2) and αN(i,i+3) correlations to the Leu[5]$C^{\alpha}H$ are clearly evident.

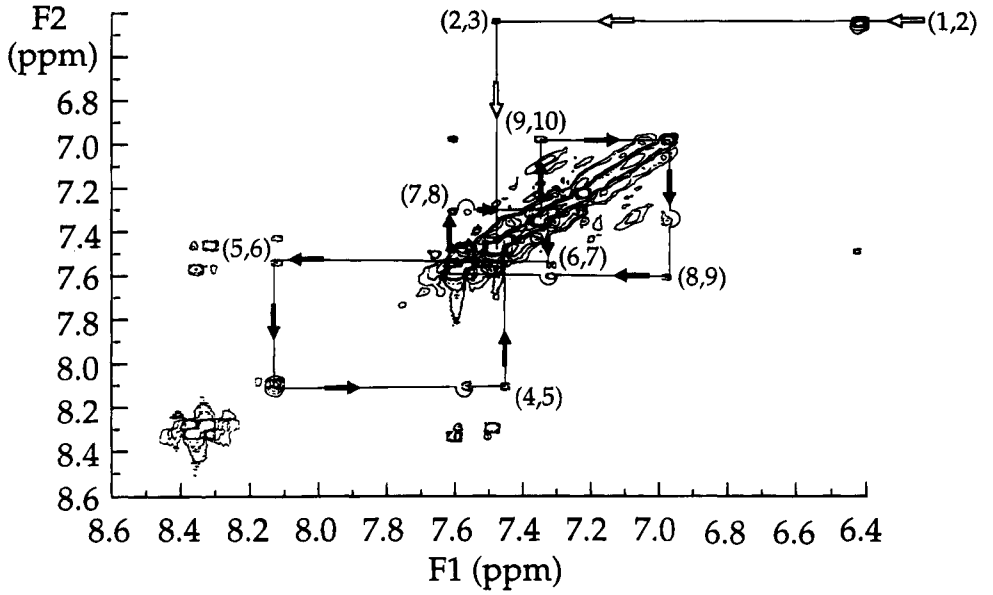

FIGURE 5: Selected section of the 500-MHz 2D ROESY spectrum of Dk[4][7/9] in $CDCl_3$ at 20 °C showing the amide and aromatic proton region. The chain of sequential NN(i,i+1) correlations beginning at the C-terminus is shown by solid arrows. The chain of sequential NN(i,i+1) correlations beginning at the N-terminus is shown by open arrows. It should be noted that the observed (1,2) correlation is not within the range shown in this figure.

Table 2: ROESY NN Cross-Peak Intensities for Dk[4][7/9] ([i]Boc-Aib[1]-Aib[2]-Aib[3]-DkNap[4]-Leu[5]-Aib[6]-Ala[7]-Aib[8]-Aib[9]-NH[10]$CH_2CH_2OCH_3$) in $CDCl_3$ at 20 °C

amide proton, i to i+1	integrated cross-peak volume[a,b]
Aib[1]NH−Aib[2]NH	−2.10/−2.29
Aib[2]NH−Aib[3]NH[c]	−4.98/−4.31
DkNap[4]NH−Leu[5]NH	−8.71/−6.46
Leu[5]NH−Aib[6]NH	−9.71/−10.14
Aib[6]NH−Ala[7]NH	−7.12/−8.65
Ala[7]NH−Aib[8]NH	−7.72/−7.90
Aib[8]NH−Aib[9]NH	−9.81/−9.20
Aib[9]NH−NH[10]	−13.56/−13.06

[a] In relative units for a mixing time of 370 ms. [b] Intensities for both the upper left and lower right cross-peaks of the 2D ROESY spectrum are given. Differences between any two such numbers may arise from nonidealities due to the technical differences between the t_1 and t_2 dimensions. [c] The Aib[3]NH and Aib[4]NH resonances are too close to observe a cross-peak between them at 500 MHz.

Table 3: C[α]H−NH Region ROESY Cross-Peak Intensities for Dk[4][7/9] ([i]Boc-Aib[1]-Aib[2]-Aib[3]-DkNap[4]-Leu[5]-Aib[6]-Ala[7]-Aib[8]-Aib[9]-NH[10]$CH_2CH_2OCH_3$) in $CDCl_3$ at 20 °C

C[α]H−NH	integrated cross-peak volume[d]
Leu[5]C[α]H−Leu[5]NH	−11.96/−9.29
Leu[5]C[α]H−Aib[6]NH	−1.42/−0.74
Ala[7]C[α]H−Ala[7]NH + Ala[7]C[α]H−NH[10] + Leu[5]C[α]H−Ala[7]NH[a]	−20.46/−18.73
Ala[7]C[α]H−Aib[8]NH + Leu[5]C[α]H−Aib[8]NH[b]	−4.80/−1.05
Ala[7]C[α]H−Aib[9]NH[c]	−1.70/−1.18

[a] The Leu[5]C[α]H−Ala[7]NH cross-peak is distinctly present above the large Ala[7]C[α]H−Ala[7]NH but cannot be integrated independently. [b] Leu[5]C[α]H−Aib[8]NH is indeed observed. However, combined intensities are reported because they cannot be integrated separately. [c] For helical peptides, this cross-peak should be observable only for 3_{10}-helices. [d] See footnote *b* of Table 2.

Leu[5]C[α]H−Aib[8]NH is indeed observed. Cross-peaks due to αN(i,i+4) correlation are characteristic of the α-helix (d = 4.2 Å), whereas those arising from αN(i,i+2) correlations are stronger in a 3_{10}-helix (d = 3.8 Å) than in an α-helix (d = 4.4 Å) (Wüthrich, 1986). If the backbone were α-helical, neither the weak αN(i,i+4) nor the yet weaker αN(i,i+2) correlation should be observed, as they would be yet longer ranged than the NN(i,i+2), none of which are observed in the ROESY spectrum [d_{NN}(i,i+2) for both the helical forms are similar, $d \sim 4.2$ Å]. On the other hand, a 3_{10}-helical conformation would be characterized by observation of αN(i,i+2) correlations which are stronger than NN(i,i+2) or αN(i,i+4) correlations. The αN(i,i+2) cross-peak between the Leu[5]C[α]H and Ala[7]NH is definitely observed despite the nearby very strong intraresidue Ala[7]C[α]H and Ala[7]NH cross-peaks. However, the only possible αN(i,i+4) cross-peak, that between the Leu[5]C[α]H and Aib[9]NH, is very weak, if present at all. The medium-ranged data are summarized in Figure 3. The corresponding αN(i,i+2) and αN(i,i+3) cross-peaks from Ala[7]C[α]H are found to be weaker than those from Leu[5]C[α]H. Table 3 presents the observed cross-peak intensities. Observation of αN(i,i+2) cross-peaks stronger than NN(i,i+2) and αN(i,i+4) cross-peaks supports the 3_{10}-helical conformation and is incompatible with an α-helical conformation. This entire concordance of evidence for 3_{10}-helicity is exactly parallel to the observations on the Nap[3]Phe[6][6/8] peptide (Basu & Kuki, 1993).

Pure Aib peptides are expected to have equal populations of both left- and right-handed helices. The presence of mono-α-alkylated, chiral residues biases one handedness of the helix over the other. Because of the presence of two L-amino acids in the peptide studied, the helix is expected to be right-handed. This fact has been confirmed by NMR; cross-peaks between the DkNap[4]C[β] methylene protons and Ala[7]CH_3 have been clearly observed (see Table 4). This is possible only if the helix is right-handed as shown in Figure 1, since the Ala[7]CH_3 of an L-Ala in a left-handed helix would point away from DkNap and toward the C-terminus. The existence of these cross-peaks also implies the close proximity of the i and i+3 residues in Dk[4][7/9], a feature of the 3_{10}-helical form. Thus, the existence of a 3_{10}-helical form rather than an α-helical form is reaffirmed.

Temperature Dependence, Dk[4][7/9]. Table 1 compares the amide proton shifts at 20 °C of Dk[4][7/9] in $CDCl_3$ and

Table 4: Correlation of DkNap^{4}C$^\beta$H and DkNap^4 Aromatic Protons to Methyl Protons

DkNap^{4}C$^\beta$H to methyl protons	integrated cross-peak volume[d]
methylene (axial 2)[a] H to Ala^7-CH$_3$	−0.49/−8.03
methylene (equat 2)[a] H to Ala^7-CH$_3$	x[b]/−2.48
methylene (axial 1)[a] H to Ala^7-CH$_3$	x[b]/−2.37
arom (prox 1)[c] H to Aib^1-CH$_3$	−2.99/−3.08
arom (dist 1)[c] H to Aib^1-CH$_3$	−1.51/−1.51

[a] Nomenclature: axial is approximately perpendicular to the five-membered ring (incorporating the DkNapC$^\alpha$H); equatorial is approximately coplanar with this five-membered ring. There are two each of axial and equatorial methylene protons (see Figure 1); each is individually assigned, and the geminal pairs are given the same number. [b] Due to the noise in the F_1 dimension, the upper left cross-peaks were unobservable. The noise is caused by a large number of closely spaced methyl peaks around 1.5 ppm (Ala^{7}CH$_3$, 1.51 ppm). [c] Proximal is the naphthyl proton closest to the helix axis; distal is the proton further from the helix axis. There are two each of proximal and distal aromatic protons; each is individually assigned and protons *ortho* to each other are given the same number. [d] See footnote *b* of Table 2.

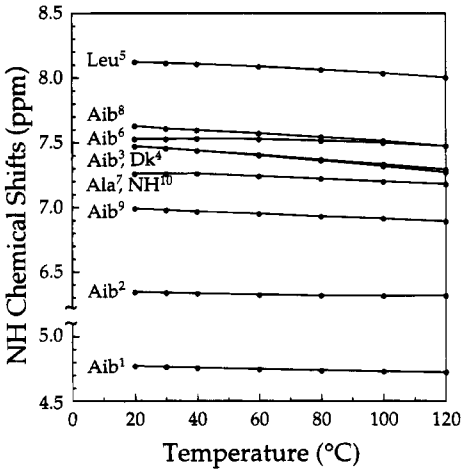

FIGURE 6: Amide proton shifts (from the 1D 400-MHz NMR spectrum) for the peptide Dk^4[7/9] in $C_2D_2Cl_4$ as a function of temperature (°C).

in the solvent ($C_2D_2Cl_4$) used for the higher temperatures. Six of the amide proton resonances can be assigned unambiguously in $C_2D_2Cl_4$, on the basis of the $CDCl_3$ results, as described in Table 1. These are the Aib^1, Aib^2, Leu^5, Ala^7, Aib^9, and the amide triplet of the C-terminal protecting group. While the amide singlets downfield from 7.4 ppm are not so easy to relate between the two solvents, it is the unambiguous assignment for Aib^1 and Aib^2 (see Table 1) that will be of pivotal importance in the temperature-dependence study.

Figure 6 presents the results of the temperature perturbation of Dk^4[7/9] in $C_2D_2Cl_4$. The striking feature of these results is the remarkable insensitivity of the amide proton shifts to temperature. The temperature coefficients of half the amide protons are less than 1 ppb/°C over the entire temperature range, while the other half fall in the range of 1−2 ppb/°C (see Table 1). One would expect significant changes in the shifts if the helix structure were disrupted to an unfolded or looser hydrogen-bonding state; the absence thereof indicates that, up to 120 °C, the helical structure of this nonamer remains stable. However, since the temperature dependence of amide proton shifts in nonpolar or weakly polar solvent is poorly understood, we sought to test this hypothesis by another method.

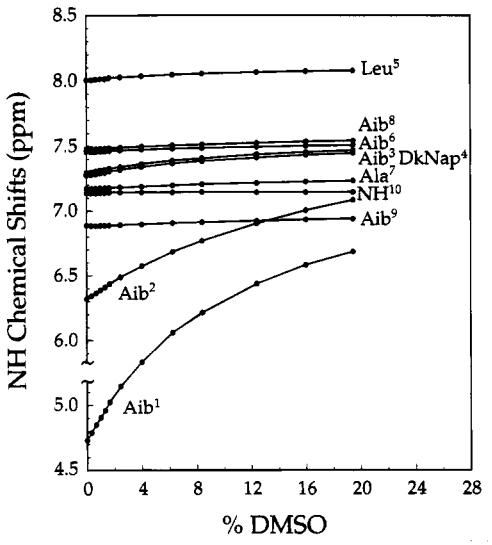

FIGURE 7: Solvent perturbation of the amide proton shifts (from the 1D 500-MHz NMR spectrum) for Dk^4[7/9] in DMSO/$C_2D_2Cl_4$ as a function of percent DMSO-d_6 at the high-temperature limit of our temperature interval, 120 °C. The markedly greater sensitivity of the two upfield amide protons makes the clear distinction between intrahelically hydrogen-bonded and free amide protons. Since the assignment of all amide resonances is established, these are in fact Aib^1 and Aib^2, and it is thereby concluded that the amides of Aib^{3,6,8,9} and the amides of DkNap^4, Leu^5, and Ala^7 are all intramolecularly hydrogen bonded at 120 °C.

Solvent Perturbation Study at High Temperatures. Solvent perturbation with DMSO-d_6 in $C_2D_2Cl_4$ was carried out directly at 120 °C. The results at this temperature (see Figure 7) show that two protons, namely, Aib^1 and Aib^2, exhibit a dramatic solvent dependence (1.4- and 0.7-ppm downfield shifts, respectively, in the range of 0−20% DMSO), while all other protons are relatively unaffected by the solvent perturbation. The strong downfield field shifts of the *free* amide protons of Aib^1 and Aib^2 upon addition of DMSO, while the other amides are protected, are precisely the classic signature of a 3_{10}-helix observed previously at room temperature (Bovey et al., 1972; Toniolo et al., 1985; Balaram et al., 1986; Basu et al., 1991) and are now observed at high temperature.

Temperature Dependence, Nap^{3}Phe^6[6/8]. The temperature dependence of the amide protons of Nap^{3}Phe^6[6/8] in DMSO-d_6 was also studied, greatly extending the temperature range previously examined (Basu et al., 1991). This is a more stringent test of the stability of the helical forms of these Aib-rich peptides because DMSO is a much stronger helix disrupter than $C_2D_2Cl_4$, due to its hydrogen-bonding ability, and because the higher boiling point of DMSO allows higher temperatures to be examined. The amide proton resonances of Nap^{3}Phe^6[6/8] from 30 to 150 °C are shown in Figure 8. Two features are striking: the linearity of all the amide proton resonances with temperature and the bimodal distribution of the slopes. The temperature coefficients ($d\delta/dT$) are given in Table 5. The amide protons of Aib^1 and Aib^2, which have been identified as the only two amide protons not involved in the intramolecular hydrogen-bonded pattern at 20 °C (Basu & Kuki, 1993), have temperature coefficients of −5.8 and −6.2 ppb/°C, respectively. These are much greater in magnitude than those of the rest of the amide protons, which range from −1.2 to −2.7 ppb/°C, and such a bimodal distribution with the first two N-terminal amides exhibiting larger temperature coefficients

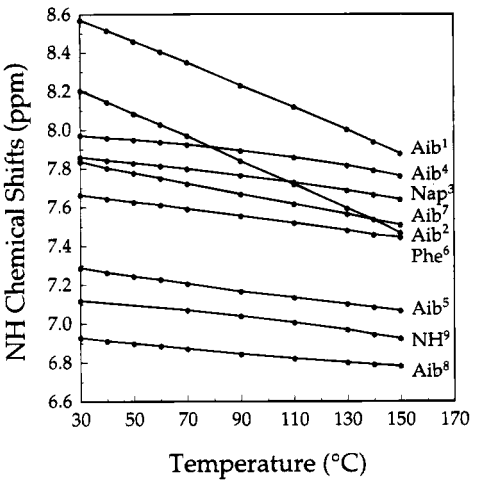

FIGURE 8: Amide proton shifts (from the 1D 400-MHz NMR spectrum) for the peptide Nap³Phe⁶[6/8] in DMSO-d_6 as a function of temperature (°C).

Table 5: Temperature Coefficients of the Amide Proton Shifts of Nap³Phe⁶[6/8] in DMSO over the Range of 30−150 °C

resonance	$\Delta\delta/\Delta T^a$	$\Delta\delta/\Delta T^b$
NH⁹	−1.6	−1.0
Aib⁸	−1.2	−1.6
Aib⁷	−2.7	−3.0
Phe⁶	−1.8	−1.5
Aib⁵	−1.8	−2.0
Aib⁴	−1.7	−1.0
Nap³	−1.8	−1.7
Aib²	−6.2	−5.2
Aib¹	−5.8	−5.1

[a] The temperature coefficient, normally defined as $d\delta/dT$, is given here by the finite difference, $\Delta\delta/\Delta T = [\delta(150\ °C) - \delta(30\ °C)]/120$ °C (in ppb/°C). [b] The temperature coefficient, normally defined as $d\delta/dT$, is given here by the finite difference, $\Delta\delta/\Delta T = [\delta(50\ °C) - \delta(30\ °C)]/20$ °C (in ppb/°C) (Basu et al., 1991; Basu & Kuki, 1993).

in DMSO is characteristic of a 3_{10}-helix. The observation that the separation of amides into this simple bimodal temperature sensitivity pattern persists over the entire temperature range is an indication that the 3_{10}-helical hydrogen-bonding pattern is preserved up to 150 °C.

DISCUSSION

A reasonable starting point in a consideration of many small and large peptides would be to assume that the dominant effect of significantly elevated temperatures would be to induce conformational transitions from lower entropy well-folded structures to more statistical coil-like structures, or at least structures exhibiting fleeting, disordered, or otherwise destabilized intramolecular hydrogen bonding. For example, temperature-dependent NMR studies have been used to analyze such transitions for peptides in both protic (Rico et al., 1986) and nonprotic weakly polar solvents (Bonora et al., 1984; Gellman et al., 1990, 1991; Dado & Gellman, 1993). Invariably in such cases, strongly nonlinear chemical shift temperature responses are observed, in contrast to the behavior of both of the peptides considered here (Figures 6 and 8).

An unfolding transition has never been observed for Aib-rich peptides or pure Aib oligomers, although these have regularly been studied up to 50−55 °C (Toniolo et al., 1985, 1991; Crisma et al., 1992). In surveying the data in the literature, one example was found of a study up to higher temperatures: the decamer *p*BrBz-$(Aib)_{10}$-O*t*Bu, prepared and studied by the Toniolo group, exhibits linear temperature-dependent shifts up to 85 °C in DMSO (Figure 4B, Toniolo et al., 1991). The significance of this result on the thermal stability is not discussed there, and the amide resonances were not sequence assigned, but it is quite clear from the body of work on pure Aib homooligomers that the thermal stability is remarkable. The steric hindrance is a relatively hard and unforgiving constraint upon the helical torsional degrees of freedom, which is decreased only slightly by increasing temperature. Interestingly, in the theoretical modeling of Aib oligopeptides (Prasad & Sasisekharan, 1979; Smythe et al., 1993; Huston & Marshall, 1994), it has been rather difficult to reproduce the pronounced experimentally observed stability of the 3_{10}-helix relative to the alternative α-helix, which probably reflects the sensitivity of the predicted conformations to the precise repulsive potential used (Paterson et al., 1981; Barone et al., 1990; Huston & Marshall, 1994). We will consider here the implications of the linear temperature behavior observed across the entire temperature range, up to 120 and 150 °C, and specifically the implications of the absence of either multiple conformations (including the α-helix) or unfolding, particularly when the slopes of the amide chemical shifts are examined.

Since the temperature-dependent NMR data reflect very different solvent interactions in the case of strongly polar solvents which hydrogen bond to the amides, on the one hand, and weakly polar solvents, on the other, these cases will be distinguished. Within a single regular backbone structure which is not undergoing a temperature-dependent conformational change, we can expect to observe the following four types of *intrinsic* (single conformation) amide chemical shift behavior, where the linearity with temperature that is evident in the data has been built in:

$$\delta_{HB}^{strong} = \delta_{residue}^{(o)} + \Delta\delta_{\mu env}^{strong}(T_o) + (d\delta_{HB}^{strong}/dT)(T - T_o) \quad (1a)$$

$$\delta_{free}^{strong} = \delta_{residue}^{(o)} + \Delta\delta_{free}^{strong}(T_o) + (d\delta_{Free}^{strong}/dT)(T - T_o) \quad (1b)$$

$$\delta_{HB}^{weak} = \delta_{residue}^{(o)} + \Delta\delta_{\mu env}^{weak}(T_o) + (d\delta_{HB}^{weak}/dT)(T - T_o) \quad (1c)$$

$$\delta_{free}^{weak} = \delta_{residue}^{(o)} + \Delta\delta_{free}^{weak}(T_o) + (d\delta_{free}^{weak}/dT)(T - T_o) \quad (1d)$$

where $\delta_{residue}^{(o)}$ is the chemical shift for the amide of a given residue type in a statistical coil (Wüthrich, 1986). The intramolecularly hydrogen-bonded amides (HB) exhibit additional shifts (at reference temperature T_o) due to their sequence position and conformational microenvironment (μenv) while immersed in strongly polar [$\Delta\delta_{\mu env}^{strong}$] or weakly polar [$\Delta\delta_{\mu env}^{weak}$] solvents, while the free or solvent-exposed amides exhibit different shifts due to their interaction with the solvent, $\Delta\delta_{free}^{strong}$ and $\Delta\delta_{free}^{weak}$. Generally speaking, it is observed that $\Delta\delta_{free}^{weak} \sim 0$, while $\Delta\delta_{free}^{strong}$ is a strong downfield shift, that $\Delta\delta_{\mu env}^{strong}$ and $\Delta\delta_{\mu env}^{weak}$ typically show only small differences for a highly stable structure such as an Aib helix, and that $(d\delta_{free}^{strong}/dT) > (d\delta_{HB}^{strong}/dT)$. This latter distinction between the temperature-dependent shift behaviors in the case of a strongly polar solvent is the frequent basis of assigning amides as intramolecularly

hydrogen bonded or free, whereas the behavior of ($d\delta^{weak}_{HB}/dT$) vs ($d\delta^{weak}_{Free}/dT$) is more subtle and is treated in the Appendix.

Thermal Stability of the Helical Structure, Nap³Phe⁶-[6/8]. Interpretation of the results of the temperature elevation studies of Nap³Phe⁶[6/8] in DMSO is straightforward. Amide protons involved in intrahelical hydrogen bonds are shielded from the lone pairs of the strongly perturbing solvent and thus exhibit markedly less temperature dependence, as has been well documented (Pitner & Urry, 1972; Vijayakumar & Balaram, 1983a,b; Balaram et al., 1986; Toniolo et al., 1985; Basu et al., 1991). Examination of Figure 8 reveals that, over the entire range of temperature studied (30−150 °C), the amide proton shifts vary linearly with temperature; thus, the temperature coefficient of each is practically constant. This is shown in Table 5, where $\Delta\delta/\Delta T$ is given for the entire temperature range (30−150 °C) and for just the first 20 °C. The temperature coefficients in Table 5 show that the amide protons of Aib¹ and Aib² exhibit significantly greater temperature dependence than the other seven amide protons in Nap³Phe⁶[6/8]. This indicates that the other seven protons remain involved in intrahelical hydrogen bonds. Furthermore, the assignment of these seven amide resonances is established, so that across the temperature range it is the identity and not just the number of intrahelical hydrogen bonds that is known. Since it has been established that Nap³Phe⁶[6/8] adopts a 3_{10}-helical structure at 30 °C, according to its 2D ROESY spectrum (Basu & Kuki, 1993), the straightforward interpretation is that it has maintained its 3_{10}-helical conformation up to 150 °C.

Thermal Stability of the Helical Structure, Dk⁴[7/9]. The interpretation of the temperature perturbation of Dk⁴[7/9] is less obvious. Since this is a temperature dependence in a weakly polar solvent ($C_2D_2Cl_4$), a clear distinction cannot be made between intrahelically hydrogen-bonded and solvent-exposed (or free) amide protons. Thus, to facilitate the interpretation of the data of Figure 6, we carried out a solvent perturbation experiment at the highest temperature studied (120 °C) by adding DMSO to the Dk⁴[7/9]/$C_2D_2Cl_4$ solution in order to determine the hydrogen-bonding pattern at that temperature. The results shown in Figure 7 reveal that the chemical shifts of the two amide protons of Aib¹ and Aib² change markedly more than those of the other amide protons. This solvent perturbation experiment at 120 °C makes the clear distinction between intrahelically hydrogen-bonded and free amide protons and is independent of the interpretive procedure normally used to rationalize the temperature response (eq 1). Just as in the solvent perturbation experiment at room temperature (Bindra & Kuki, 1994), this absence of intrahelical hydrogen bonds for only Aib¹ and Aib² is consistent with a 3_{10}-helical conformation. Furthermore, since the 2D ROESY spectrum in $CDCl_3$ demonstrates that Dk⁴[7/9] adopts a 3_{10}-helical conformation at 20 °C, we conclude that Dk⁴[7/9] also retains its 3_{10}-helical conformation up to 120 °C in $C_2D_2Cl_4$.

These conclusions are also supported by the simple observation that, at any temperature within the range studied, the chemical shift dispersion of the intramolecularly hydrogen-bonded Aib amides is maintained in the case of both the nonamer Dk⁴[7/9] (Figure 6) and the octamer Nap³Phe⁶-[6/8] (Figure 8). It has been established (Wagner et al., 1983) that differing intramolecular hydrogen bond lengths can generate ample chemical shift dispersion, and other local influences are also likely to be present (Wishart et al., 1991). The microenvironment-induced differences of amide chemical shifts, $\Delta\delta^{strong}_{\mu env}$ and $\Delta\delta^{weak}_{\mu env}$, give rise to a 0.6 ppm chemical shift dispersion among the Aib amides in Dk⁴-[7/9] and a 1 ppm chemical shift dispersion among the Aib amides in Nap³Phe⁶[6/8], at normal temperatures, and this dispersion is preserved at the greatly elevated temperatures.

This retention of the 3_{10}-helical conformation of both peptides over the entire temperature range studied implies that these Aib-rich peptides are remarkably conformationally quiet. Typically, peptides of such short length would exist in a number of marginally stable conformations, and a yet larger range of conformations would become accessible with, say, 50 °C increases in temperature. In such general cases, temperature-induced conformational transitions are then expected, so that the chemical shift for each proton will of course not reflect the behavior intrinsic to a given structure. This has been demonstrated quantitatively in previous analyses; in particular, see eq 1 of Rico et al. (1986); this is a study in which the thermal unfolding of the S-peptide was observed by monitoring the NMR of (side-chain) protons. For both the Nap³Phe⁶[6/8] and Dk⁴[7/9] peptides, however, the 3_{10}-helical conformation has been observed to persist to high temperatures. The temperature coefficients in Tables 1 and 5 are therefore interpreted as *intrinsic* temperature dependences of these 3_{10}-helical backbone structures. These coefficients and their linearity are then benchmarks for the underlying intrinsic temperature dependence of helical amides in these four environments (see Appendix). The high-temperature stability is also expected to be observed in many other Aib-rich helical peptides as well, provided that the sequences are very high in Aib composition (≥70%) and possess only noncontiguous L-residues.

Helical Stability of Aib-Rich Peptides in the Context of Helix/Coil Equilibria. The extreme thermal stability of helical structures in these Aib-rich peptides in both strongly and weakly polar solvents is most likely a reflection of the absence of any true coil-like state of an Aib-rich peptide. The studies on helix/coil equilibria of an *isolated* Aib guest residue within a sequence of common amino acids are but a harbinger of this stability phenomenon (O'Neil & DeGrado, 1990; Hermans et al., 1992). The conformational energy maps for the backbone dihedral angles (ϕ,ψ) of terminally blocked Aib, and of oligomers thereof in a regular structure, have been computed and show clearly the absence of any wide basin or alternative minima other than in the 3_{10}-/α-helical region (Paterson et al., 1981). Therefore, the standard large entropy gain for a helix → coil transition is greatly reduced, and the temperature at which helix disruption will occur is concomitantly strongly raised [from a simple $d(\Delta G^{\circ}_{helix\rightarrow coil})/dT = -\Delta S^{\circ}_{helix\rightarrow coil}$ argument, with greatly reduced positive $\Delta S^{\circ}_{helix\rightarrow coil}$]. More recent simulations have addressed the entropy change $\Delta S^{\circ}_{\alpha\rightarrow 3_{10}}$ for a pure Aib homooligomer (Huston & Marshall, 1994), but this cannot complete the picture because the ΔS° for unfolding an Aib α-helix is not known (nor has a pure Aib α-helical homo-oligomer ever been observed). Nevertheless, it is undoubtedly true that, at some temperature, an Aib-rich peptide will at least undergo a transition from a 3_{10}-helix to a distribution of helical forms, where individual hydrogen bonds break and transfer (Huston & Marshall, 1994), and the conformation

Table 6: Melting Temperatures of Several *de Novo* Designed Oligopeptides

length	solvent[a]	peptide	T_m (°C)	reference
10	H_2O	$(D,L\text{-}K)_mA_{10}(D,L\text{-}K)_m$	*b*	Ingwall et al., 1968
14	H_2O	$AcY(AEAAKA)_2FNH_2$	−5[d]	Scholtz et al., 1991b
16	H_2O	$Ac(AKAAE)_3ANH_2$	<0	Marqusee & Baldwin, 1987
17	H_2O	$AcAES(AAKEA)_2AKANH_2$	11	Merutka & Stellwagon, 1990
16	H_2O	$Ac(AAAAK)_3ANH_2$	14[c]	Marqusee et al., 1989
20	H_2O	$AcY(AEAAKA)_3FNH_2$	16[d]	Scholtz et al., 1991b
17	H_2O	$AcA(EAAAK)_3ANH_2$	22	Marqusee & Baldwin, 1987; Merutka & Stellwagon, 1990
26	H_2O	$AcY(AEAAKA)_4FNH_2$	28[d]	Scholtz et al., 1991b
160	H_2O	$(D,L\text{-}K)_mA_{160}(D,L\text{-}K)_m$	29	Ingwall et al., 1968
32	H_2O	$AcY(AEAAKA)_5FNH_2$	32[d]	Scholtz et al., 1991b
38	H_2O	$AcY(AEAAKA)_6FNH_2$	35[d]	Scholtz et al., 1991b
50	H_2O	$AcY(AEAAKA)_8FNH_2$	42[d]	Scholtz et al., 1991b
450	H_2O	$(D,L\text{-}K)_mA_{450}(D,L\text{-}K)_m$	49	Ingwall et al., 1968
1000	H_2O	$(D,L\text{-}K)_mA_{1000}(D,L\text{-}K)_m$	58	Ingwall et al., 1968
8	$CDCl_3$	Z-$(Aib)_8$−O*t*Bu[e]	≥55	Toniolo et al., 1985
30	1-PrOH	$K_2GL_{24}K_2ANH_2$[f]	≥70	Davis et al., 1983
10	DMSO	*p*BrBz−$(Aib)_{10}$−O*t*Bu[g]	≥85	Toniolo et al., 1991
9	$C_2D_2Cl_4$	$Dk^4[7/9]$[h]	≥120	this work
8	DMSO	$Nap^3Phe^6[6/8]$[i]	≥150	this work

[a] See text for discussion of the significance of solvent effects in comparing T_m. [b] Not helical above 0 °C. [c] See Vila et al. (1992) for additional discussion of these data. [d] Read from Figure 3, Scholtz et al., 1991b. [e] See Figure 7, Toniolo et al., 1985. [f] See Figure 3, Davis et al., 1983. This is an interesting example of a long peptide, designed for trans-bilayer studies, which exhibits high thermal stability in 1-propanol. [g] See Figure 4B, Toniolo et al., 1991. [h] $Dk^4[7/9]$ is a 77% Aib-class peptide, where Aib class includes Aib and DkNap. [i] $Nap^3Phe^6[6/8]$ is a 75% Aib peptide: Ac-$(Aib)_2$-Nap-$(Aib)_2$-Phe-$(Aib)_2$-NHMe.

floats over the closely related minima in the potential energy surface corresponding to the 3_{10}- and α-helical structures. However, that point has not yet been reached, and it is remarkable that temperatures of 120 and 150 °C do not even begin this process by introducing at least one defect into the 3_{10} hydrogen-bonding pattern.

This thermal stability can be contrasted with that of aqueous solutions of peptides containing primarily alanine. Quite a number of such alanine-rich peptides have been studied to date, where typically lysine and glutamate have been included to achieve water solubility (Ingwall et al., 1968; Marqusee & Baldwin, 1987; Marqusee et al., 1989; Bradley et al., 1990; Merutka & Stellwagon, 1989, 1990; Merutka et al., 1993; Liff et al., 1991; Scholtz et al., 1991a,b, 1993; Rohl et al., 1992; Vila et al., 1992; Chakrabartty et al., 1994). The thermal stabilities, as measured by the melting temperature [where K_{eq} = [coil]/[helix] = 1], of several alanine oligopeptides are compared in Table 6 to those of Aib-rich peptides. It can be seen that, even at a length of 50, in water, the alanine-rich peptides with rather stable helical sequences have yet to attain the thermal stabilities of Aib-rich peptides of length 8, in DMSO.

Clearly, the effect of solvent on thermal stability must be addressed in making even qualitative comparisons between these results. Water is a more helix-disruptive environment, because it can both donate and accept protons in the formation of hydrogen bonds, whereas DMSO can act strongly only an an acceptor, and $C_2D_2Cl_4$ can act as neither. However, the case of DMSO deserves closer inspection. Initially, in a 3_{10}-helix of, say, nine amides, there are seven intrahelical hydrogen bonds and two hydrogen bonds to the solvent. Since the DMSO solvent does not hydrogen bond to itself, unfolding of the helix will cause a replacement of seven intrahelical hydrogen bonds by seven new hydrogen bonds to the solvent and no loss of DMSO−DMSO hydrogen bonding. The net result is no loss in the total number of hydrogen bonds upon unfolding, exactly the same results as in water (in water, 14 old hydrogen bonds are replaced by 14 new hydrogen bonds). Hence, while there can still be marked solvent effects, the most relevant comparison is between the data in DMSO and that in water. DMSO has indeed been documented as a solvent which can disrupt the hydrogen-bonding pattern of Aib-containing peptides at room temperature; these examples, however, pertain to a peptide with just under 50% Aib composition (Vijayakumar & Balaram, 1983a) and one with contiguous L-amino acids (Balaram et al., 1986). We have recently observed and analyzed another example in a sequence possessing contiguous L-amino acids, in which the hydrogen bonding in the room temperature structure is weakened by DMSO, relative to that in the much less polar $CDCl_3$ solvent (Pettijohn & Kuki, 1995). The data from the present work (with only isolated L-amino acids) and from the Toniolo group (Table 6), however, provide no indication of an effect of the substitution of DMSO-d_6 for the $C_2D_2Cl_4$ solvent. Even though the hydrogen-bonding capacity of DMSO qualitatively approaches that of water, DMSO has no observable effect on the extreme thermal stability observed for the Aib-rich helices at the temperatures examined. More experiments on different Aib-rich peptides and particularly with sequences redesigned for aqueous solubility are clearly needed to establish the thermodynamics and the role of solvent quantitatively. These experiments are being pursued in our laboratory.

CONCLUSION

The $Dk^4[7/9]$ Aib-rich peptide has been shown to have a three-dimensional structure which is compatible with a stable, full-length 3_{10}-helix and not with an α-helix, at 20 °C. This demonstrates that the Aib-rich sequence of this [7/9] Aib-class peptide with noncontiguously placed Leu and Ala continues to yield a 3_{10}-helix, as in the Aib octamer Nap^3-$Phe^6[6/8]$ studied by ROESY earlier (Basu et al., 1991; Basu & Kuki, 1993).

The 3_{10}-helical structures of the two Aib-rich peptides studied here are found to possess remarkable thermal stability. The helix structure is maintained to well over 100

°C in both strongly and weakly polar solvents. The hydrogen-bonding pattern of Dk[4][7/9] is 3_{10}-helical as observed directly at 120 °C. While the quantitation of $\Delta S^{\circ}_{\text{helix}\rightarrow\text{coil}}$ has not been achieved, it is apparent that this is greatly reduced relative to that of non-Aib peptides, in accordance with the considerable body of evidence on the steric hindrance due to the *gem*-dimethyl group. Yet, theoretical studies (Prasad & Sasisekharan, 1979; Paterson et al., 1981; Barone et al., 1990; Hermans et al., 1992; Huston & Marshall, 1994) pertinent to the effect of the steric hindrance upon this entropy change do not enable one to predict such a wide thermal range of helical stability. The theoretical challenge is considerably exacerbated by the sensitive dependence upon the exact model of repulsive interactions employed. In particular, the experimentally observed resistance of these peptides to even the limited conformational mobility of one or several ruptured hydrogen bonds is perhaps the most striking result, since the detailed and assigned hydrogen-bonding pattern is verified to be 3_{10}-helical at 120 °C. This extreme thermal stability indicates that these Aib-rich sequences are well suited as a strategy for creating well-defined scaffolding in peptides permitting the inclusion of both guest L-amino acids and cyclically locked Aib-class guest amino acids. This research into the molecular design of families of stable 3_{10}-helices is being pursued with recently available synthetic aromatic amino acids designed to share the same backbone helical propensity (Kotha et al., 1992). In addition, the elucidation of the thermodynamic conditions enabling such thermal stability may well be of general interest in the design of helical and multihelical peptide and protein structures.

APPENDIX

Temperature Dependence of Amide Proton Shifts within a Stable Helical Structure. The conformationally quiet nature of these peptides allows us to interpret more fully the temperature coefficients of the amide proton shifts of these peptides in a weakly polar solvent. Free amide protons have a large downfield shift in DMSO at room temperature, which is then reduced with the increasing thermal motion of the solvent molecules to yield a large negative ($d\delta^{\text{strong}}_{\text{free}}/dT$). In weakly polar solvents the free amide protons do not experience the strong downfield shift and hence tend to be the most upfield amides, with weak ($d\delta^{\text{weak}}_{\text{free}}/dT$) ~ ($d\delta^{\text{weak}}_{\text{HB}}/dT$).

Stevens et al. (1980) studied the temperature dependence of amide proton shifts of terminally blocked amino acids, as well as of di- and tripeptides, as models of "free" amide protons. They found that the average of the temperature coefficients of these free amide protons in $CDCl_3$ was −2.4 ± 0.5 ppb/°C. They also reported that intramolecularly hydrogen-bonded amide protons exhibited similarly small temperature coefficients. In a subsequent report, Bonora et al. (1984) examined Aib trimers, tetramers, and pentamers and determined that amide protons which participated in hydrogen bonds that were thermally disrupted (either by conformational changes or by a lessening of an aggregation) exhibit larger chemical shift temperature coefficients in $CDCl_3$ [see also the concentration-dependent temperature coefficients documented in Toniolo et al. (1985)].

Since the nonamer Dk[4][7/9] does not exhibit such conformational equilibria, we can compare the temperature coefficients of the free and intrahelically hydrogen-bonded amides as revealing the behaviors of $\delta^{\text{weak}}_{\text{free}}$ and $\delta^{\text{weak}}_{\text{HB}}$, respectively, intrinsic to a single conformation. The free protons of Aib^1 and Aib^2 have the *smallest* temperature coefficients; $d[\delta^{\text{weak}}_{\text{free}}]/dT$ = −0.3 and −0.5 ppb/°C (see Table 1). These values for free amide protons in $C_2D_2Cl_4$ are much less than those (−2.4 ± 0.5 ppb/°C) reported by Stevens et al. (1980). The solvent-exposed (free) amides of those di- and tripeptides, however, are free in statistical coil conformations which is not the same as being free at the N-terminus of a helix; hence, these do not correspond to *any* of the four types examined here. The approximately 5-fold greater temperature coefficient most likely reflects the considerable variation in microenvironments experienced in a statistical coil state, even in the weakly polar solvent. Put another way, we would have expected similar −2.4 ppb/°C behavior for the amides of the N-terminal Aib^1 and Aib^2 in Dk[4][7/9] if the helical conformation had unfolded. Hence, the observation of very low chemical shift temperature dependencies, $d[\delta^{\text{weak}}_{\text{free}}]/dT$, may be an important general indicator of the absence of conformational equilibria.

The intrahelically hydrogen-bonded amide protons exhibit temperature coefficients, $d[\delta^{\text{weak}}_{\text{HB}}]/dT$, which range from −0.6 to −1.8 ppb/°C (Table 1). While the differences are small, there does appear to be a distinction between free and hydrogen-bonded amide protons in the weakly polar solvent. The greater temperature dependence of the hydrogen-bonded protons may be a result of increasing excitation of the hydrogen bond stretching vibration with temperature, as described by Muller and Reiter (1965). Hydrogen bond stretching frequencies are much lower than covalently bonded vibration frequencies, and hence excited vibrational states are appreciably populated at room temperature. Thus, an increase of temperature leads to a change in the population distribution of the hydrogen bond vibrations. Anharmonicity of the hydrogen bond stretching potential then leads to changes in the average O···H separation, which will in turn lead to a lessening of the downfield perturbation of the NH shift. Muller and Reiter found reasonable agreement between their calculated temperature coefficients of −2 to −3 ppb/°C and the data on the intermolecular hydrogen-bonded systems that they had studied (acetic acid dimers and acetic acid−acetone). Furthermore, this vibrational excitation mechanism evidently has greater influence upon the hydrogen-bonded amide proton shifts $\delta^{\text{weak}}_{\text{HB}}$ than the nonpolar or weakly polar solvent has upon the exposed amide proton shifts $\delta^{\text{weak}}_{\text{free}}$. As a result, it is the solvent-exposed amide protons at the N-terminus, viz., those of Aib^1 and Aib^2 (Table 2), which exhibit the *smallest* temperature coefficients, in striking contrast to the case in polar hydrogen-bonding solvents.

This vibrational excitation mechanism is clearly a subtle effect within a usually considerably more conformationally dynamic situation; it is more compelling since the simple linear behavior is observed over the wide temperature range studied, which would be expected to reveal any conformational complexities if present.

The enhancement of ($d\delta^{\text{weak}}_{\text{HB}}/dT$) over ($d\delta^{\text{weak}}_{\text{free}}/dT$), as implied by the Muller and Reiter mechanism, had not been observed in the Aib oligomer series [n = 1−12; Toniolo et al., 1985; see also Toniolo et al. (1988)], where the values of ($d\delta^{\text{weak}}_{\text{Free}}$/dT) are between −1.3 and −5.2 ppb/°C for

lengths ($n = 8-10$) comparable to the present work, while the corresponding ($d\delta_{HB}^{weak}/dT$) coefficients were also found to fall within this same interval.

REFERENCES

Altmann, K.-H., Wójcik, J., Vásquez, M., & Scheraga, H. A. (1990) *Biopolymers 30*, 107−120.

Balaram, H., Sukumar, M., & Balaram, P. (1986) *Biopolymers 25*, 2209−2223.

Barone, V., Fraternali, F., & Cristinziano, P. L. (1990) *Macromolecules 23*, 2038−2044.

Basu, G., & Kuki, A. (1992) *Biopolymers 32*, 61−71.

Basu, G., & Kuki, A. (1993) *Biopolymers 33*, 995−1000.

Basu, G., Bagchi, K., & Kuki, A. (1991) *Biopolymers 31*, 1763−1774.

Basu, G., Anglos, D., & Kuki, A. (1993) *Biochemistry 32*, 3067−3076.

Bax, A., & Davis, D. G. (1985) *J. Magn. Reson. 63*, 207−213.

Bindra, V. A., & Kuki, A. (1994) *Int. J. Pept. Protein Res. 44*, 539−548.

Bonora, G. M., Mapelli, C., Toniolo, C., Wilkening, R. R., & Stevens, E. S. (1984) *Int. J. Biol. Macromol. 6*, 179−188.

Bothner-By, A. A., Stephens, R. L., Lee, J.-M., Warren, C. D., & Jeanloz, R. W. (1984) *J. Am. Chem. Soc. 106*, 811−813.

Bovey, F. A., Brewster, A. I., Patel, D. J., Tonelli, A. E., & Torchia, D. A. (1972) *Acc. Chem. Res. 5*, 193−200.

Bradley, E. K., Thomason, J. F., Cohen, F. E., Kosen, P. A., & Kuntz, I. D. (1990) *J. Mol. Biol. 215*, 607−622.

Chakrabartty, A., Kortemme, T., & Baldwin, R. L. (1994) *Protein Sci. 3*, 843−852.

Crisma, M., Anzolin, M., Bonora, G. M., Toniolo, C., Benedetti, E., Di Blasio, B., Pavone, V., Saviano, M., Lombardi, A., Nastri, F., & Pedone, C. (1992) *Gazz. Chim. Ital. 122*, 239−244.

Dado, G. P., & Gellman, S. H. (1993) *J. Am. Chem. Soc. 115*, 4228−4245.

Davis J. H., Clare, D. M., Hodges, R. S., & Bloom, M. (1983) *Biochemistry 22*, 5298−5305.

Di Blasio, B., Pavone, V., Lombardi, A., Pedone, C., & Benedetti, E. (1993) *Biopolymers 33*, 1037−1049.

Gellman, S. H., Adams, B. R., & Dado, G. P. (1990) *J. Am. Chem. Soc. 112*, 460−461.

Gellman, S. H., Dado, G. P., Liang, G.-B., & Adams, B. R. (1991) *J. Am. Chem. Soc. 113*, 1164−1173.

Hermans, J., Anderson, A. G., & Yun, R. H. (1992) *Biochemistry 31*, 5646−5653.

Huston, S. E., & Marshall, G. R. (1994) *Biopolymers 34*, 75−90.

Ingwall, R. T., Scheraga, H. A., Lotan, N., Berger, A., & Katchalski, E. (1968) *Biopolymers 6*, 331−368.

Karle, I. L., & Balaram, P. (1990) *Biochemistry 29*, 6747−6756.

Kotha, S., Anglos, D., & Kuki, A. (1992) *Tetrahedron Lett. 33*, 1569−1572.

Liff, M. I., Lyu, P. C., & Kallenbach, N. R. (1991) *J. Am. Chem. Soc. 113*, 1014−1019.

Marqusee, S., & Baldwin, R. L. (1987) *Proc. Natl. Acad. Sci. U.S.A. 84*, 8898−8902.

Marqusee, S., Robbins, V. H., & Baldwin, R. L. (1989) *Proc. Natl. Acad. Sci. U.S.A. 86*, 5286−5290.

Marshall, G. R., Hodgkin, E. E., Langs, D. A., Smith, G. D., Zabrocki, J., & Leplawy, M. T. (1990) *Proc. Natl. Acad. Sci. U.S.A. 87*, 487−491.

Merutka, G., & Stellwagen, E. (1989) *Biochemistry 28*, 352−357.

Merutka, G., & Stellwagen, E. (1990) *Biochemistry 29*, 894−898.

Merutka, G., Morikis, D., Brüschweiler, R. & Wright, P. E. (1993) *Biochemistry 32*, 13089−13097.

Muller, N., & Reiter, R. C. (1965) *J. Chem. Phys. 42*, 3265−3269.

O'Neil, K. T., & DeGrado, W. F. (1990) *Science 250*, 646−651.

Paterson, Y., Rumsey, S. M., Benedetti, E., Némethy, G., & Scheraga, H. A. (1981) *J. Am. Chem. Soc. 103*, 2947−2955.

Pettijohn, A., & Kuki, A. (1995) *Biopolymers* (submitted for publication).

Piantini, U., Sørensen, O. W., & Ernst, R. R. (1982) *J. Am. Chem. Soc. 104*, 6800−6801.

Pitner, T. P., & Urry, D. W. (1972) *J. Am. Chem. Soc. 94*, 1399−1400.

Prasad, B. V. V., & Sasisekharan, V. (1979) *Macromolecules 12*, 1107−1110.

Prasad, B. V. V., & Balaram, P. (1984) *CRC Crit. Rev. Biochem. 16*, 307−348.

Rico, M., Santoro, J., Bermejo, F. J., Herranz, J., Nieto, J. L., Gallego, E., & Jiménez, M. A. (1986) *Biopolymers 25*, 1031−1053.

Rohl, C. A., Scholtz, J. M., York, E. J., Stewart, J. M., & Baldwin, R. L. (1992) *Biochemistry 31*, 1263−1269.

Scholtz, J. M., Marqusee, S., Baldwin, R. L., York, E. J., Stewart, J. M., Santoro, M., & Bolen, D. W. (1991a) *Proc. Natl. Acad. Sci. U.S.A. 88*, 2854−2858.

Scholtz, J. M., Qian, H., York, E. J., Stewart, J. M., & Baldwin, R. L. (1991b) *Biopolymers 31*, 1463−1470.

Scholtz, J. M., Qian, H., Robbins, V. H., & Baldwin, R. L. (1993) *Biochemistry 32*, 9668−9676.

Slomczynska, U., Beusen, D. D., Zabrocki, J., Kociolek, K., Redlinski, A., Reusser, F., Hutton, W. C., Leplawy, M. T., & Marshall, G. R. (1992) *J. Am. Chem. Soc. 114*, 4095−4106.

Smythe, M. L., Huston, S. E., & Marshall, G. R. (1993) *J. Am. Chem. Soc. 115*, 11594−11595.

Stevens, E. S., Sugawara, N., Bonora, G. M., & Toniolo, C. (1980) *J. Am. Chem. Soc. 102*, 7048−7050.

Toniolo, C., Bonora, G. M., Barone, V., Bavoso, A., Benedetti, E., Di Blasio, B., Grimaldi, P., Lelj, F., Pavone, V., & Pedone, C. (1985) *Macromolecules 18*, 895−902.

Toniolo, C., Borona, G. M., Formaggio, F., Crisma, M., Bavoso, A., Benedetti, E., Di Blasio, B., Pavone, V., & Pedone, C. (1988) *Gazz. Chim. Ital. 118*, 47−53.

Toniolo, C., Crisma, M., Bonora, G. M., Benedetti, E., Di Blasio, B., Pavone, V., Pedone C., & Santini, A. (1991) *Biopolymers 31*, 129−138.

Vijayakumar, E. K. S., & Balaram, P. (1983a) *Tetrahedron 39*, 2725−2731.

Vijayakumar, E. K. S., & Balaram, P. (1983b) *Biopolymers 22*, 2133−2140.

Vila, J., Williams, R. L., Grant, J. A., Wójcik, J., & Scheraga, H. A. (1992) *Proc. Natl. Acad. Sci. U.S.A. 89*, 7821−7825.

Wagner, G., Pardi, A., & Wüthrich, K. (1983) *J. Am. Chem. Soc. 105*, 5948−5949.

Wishart, D. S., Sykes, B. D., & Richards, F. M. (1991) *J. Mol. Biol. 222*, 311−333.

Wójcik, J., Altmann, K.-H., & Scheraga, H. A. (1990) *Biopolymers 30*, 121−134.

Wüthrich, K. (1986) *NMR of Proteins and Nucleic Acids*, pp 117−129, Wiley, New York.

BI941099N